Scattering Characteristics of Two-Dimensionally Periodic Impedance Surface

Ruey Bing Hwang, *Member, IEEE*

Abstract—We present here an exact formulation for the three-dimensional (3-D) boundary-value problem of plane wave scattering by a two-dimensionally (2-D) periodic impedance surface in a uniform medium. The scattering characteristics of such a structure are rigorously analyzed in terms of the complete set of both TE- and TM-polarized plane waves in the uniform medium. Extensive numerical results are given to illustrate physical phenomena associated with the structure.

Index Terms—Impedance boundary condition, periodic impedance boundary condition, scattering and diffraction, two-dimensionally (2-D) periodic impedance surface.

I. Introduction

THE scattering of waves by periodic structures has long been a subject of continuing interest, and extensive theoretical and experimental results are available in the literature [1]–[4]. Over the past few decades, two-dimensional (2-D) frequency-selective surfaces (FSSs) have found numerous aspects of applications [5]–[7]. In particular, the class of 2-D periodic structures that are also known as the photonic bandgap (PBG) structures has attracted considerable attention in recent years [8]–[10]. Many authors have presented the analysis of planar structure consisting of multiple gratings. To mention a few, a pair of perfectly conducting lamellar transmission gratings separated in space and oriented with orthogonal periodicity were analyzed, with detailed numerical data for use as a solar-selected element [11]. Multilayered periodic structures had been analyzed on the basis of the generalized scattering matrix theory [12]. Scattering characteristics of 2-D photonic crystals modeled by a finite stack of dielectric grids of infinite extension were studied by using integral theory [8]. Noponen, *et al.* [13], synthesized 2-D periodic structures to achieve $1 \times N$ beam splitters of the transmission type. A rigorous treatment of scattering characteristics of bigratings has been reported, with some potential applications proposed [14]. The transmission response was tailored by the synthesis of finite artificial lattices carrying passive metal-dielectric unit cells [15]. Most of the research listed above is based on a rigorous formulation and needs large computer resources. On the other hand, the *impedance boundary condition* (IBC) approximation

is an effective way to model complex structures [16]–[20]; it replaces the original complex structure with surface impedance so that the problem complexity can be greatly reduced. For example, Su and Ling [20] utilized the genetic algorithm to determine the equivalent impedance boundary condition for material-coated corrugated gratings. Furthermore, Wait [16] had shown that the IBC is not only applicable to a medium having a large refractive index, but also is suitable for layered media, embedded wire grids, and even layers in which the contrast in refractive index approaches unity. In fact, the case of a one-dimensionally (1-D) periodic reactive surface had been employed successfully as a model for the analysis of wave phenomena associated with periodic structures; for the first time, Wood's anomalies were then explained on a rigorous basis [2]. The guidance characteristics of surface waves along a corrugated surface have been thoroughly studied by many authors by using the model of impedance surface [24]–[26], while some new and interesting guidance characteristics of 2-D periodic impedance surface have been examined recently [20]. Since the equivalent impedance boundary conditions are well studied for some canonical structures, including the periodic ones [21]–[23], we concentrate here on the study of the scattering characteristics of the 2-D periodic surface impedance that will be expressed in terms of a double Fourier series.

Specifically, we present in this paper an algorithm for analyzing 2-D periodic multilayer structures that are characterized by *periodic IBCs*, with a particular attention paid to the relationship between their scattering and guiding characteristics. Such a model is intended for the study of wave phenomena associated with 2-D periodic structures. It had been shown [20] that the case of impedance surface can be formulated rigorously by the method of mode matching as a three-dimensional (3-D) electromagnetic (EM) boundary-value problem. The total fields above the planar impedance surface can be expressed in the form of double Fourier series, with each space harmonic appearing as a plane wave consisting of both TE and TM constituent plane waves. After invoking the periodic impedance boundary condition on the planar surface, the input–output relations between the incident and reflected waves can be obtained and then the scattering characteristics will be also realized.

Based on the exact approach described above, we have carried out extensive numerical results to identify and explain physical phenomena associated with the 2-D periodic impedance surface. In particular, Wood's anomalies have been carefully examined, in contrast to those in the case of 1-D periodic cases. Furthermore, potential applications are suggested such as that the 2-D lossy periodic impedance surface may provide more frequency bands to absorbed the energy of an incident wave.

The author is with Microelectronics and Information Systems Research Center, National Chiao Tung University, Hsinchu, Taiwan, R.O.C. (e-mail: rbhwang@eic.nctu.edu.tw).

Publisher Item Identifier S 0018-926X(00)09346-7.

II. STATEMENT OF PROBLEM

The approximation of impedance boundary condition can be realized by examining a popular structure, the corrugated surface, which has been thoroughly studied in various textbooks and articles [24]–[26]. For example, a corrugated metal slab has a series of vertical slots, as shown in Fig. 1. Each slot can be regarded as a parallel-plate waveguide with a short-circuit termination. At the top surface of the corrugated metal slab, there are two alternating regions in each unit cell; one is the metal surface and the other is an air opening. The former acts as a short circuit, while the latter contains the effect of all the modes of the parallel-plate waveguide. Thus, an equivalent impedance may be assigned to replace the structure underneath the top surface; hence, the top surface can be regarded as having a periodic variation of the impedance.

Referring to Fig. 2, the interface between the air region and the periodic layer can be viewed as an impedance surface for the fields in the air region. Such a surface impedance depends on the physical as well as structural parameters below the surface. Fig. 3 depicts the scattering of a plane wave by a planar impedance surface that is periodic in two dimensions. For simplicity, the space above the surface is taken to be air of infinite extent. Such a structure is intended as a model for the study of wave phenomena associated with the class of multilayer periodic structures. In the literature, the case of 1-D periodic reactive surface had been successfully employed as a model for the analysis of wave phenomena associated with periodic structures; for the first time, Wood's anomalies were explained on a rigorous basis [2]. As an extension, we consider here a periodically perturbed surface impedance with the spatial variation given by

$$Z(x, y) = Z_s \left[1 + 2\delta_x \cos \frac{2\pi x}{a} + 2\delta_y \cos \frac{2\pi y}{b} \right.$$
$$\left. + 4\delta_{xy} \cos \frac{2\pi x}{a} \cos \frac{2\pi y}{b} \right] \quad (1)$$
$$Z_s = R_s + jX_s. \quad (2)$$

Here, Z_s is the average surface impedance, with the surface resistance R_s and the surface reactance X_s; δ_x, δ_y, and δ_{xy} are the modulation indexes; a and b are the periods in the x- and y-direction, respectively. Such a characterization may be regarded as the first-order approximation of a double Fourier series for a general 2-D periodic surface impedance; if needed, more terms may be included and the ensuing analysis can still be applied. We observed that the scattering problem posed here may be analyzed rigorously, as explained in Section III.

III. METHOD OF ANALYSIS

Referring to Fig. 3, an incident plane wave is scattered by the 2-D periodic impedance surface and a set of space harmonics is generated in each of the two directions of periodic variation. In the air region, each space harmonic appears a plane wave of which the tangential field components may be generally represented as a superposition of the TE- and TM-polarized plane waves with respect to the z-direction. For the mth space harmonic in the x-direction and the nth space harmonic in the y-di-
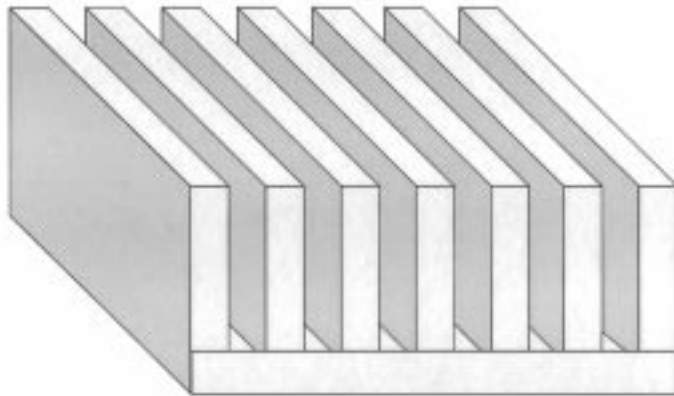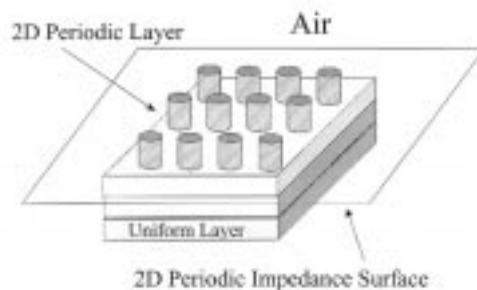

Fig. 1. Corrugated metal surface.

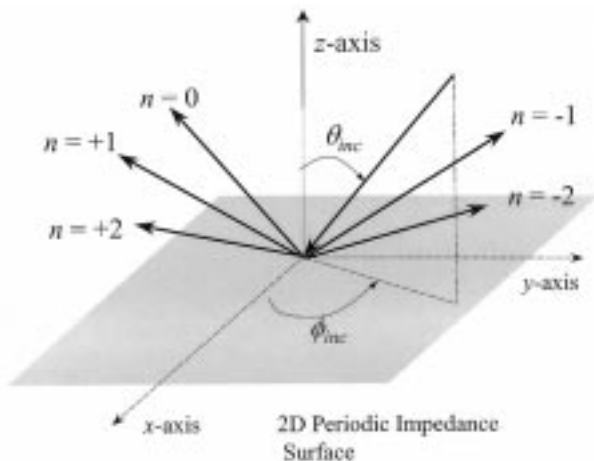Fig. 2. Typical configuration of 2-D periodic structure.

Fig. 3. Scattering of plane wave by 2-D periodic impedance surface.

rection, to be denoted by the mnth harmonic for simplicity, the tangential-field components can be written as

$$\underline{z}_o \times \underline{E}_{tmn}(\rho, z)$$
$$= [\underline{a}'_{mn} V'_{mn}(z) + \underline{a}''_{mn} V''_{mn}(z)] \cdot \exp(-j\underline{k}_{tmn} \cdot \underline{\rho}) \quad (3a)$$
$$\underline{H}_{tmn}(\rho, z)$$
$$= [\underline{a}'_{mn} I'_{mn}(z) + \underline{a}''_{mn} I''_{mn}(z)] \cdot \exp(-j\underline{k}_{tmn} \cdot \underline{\rho}) \quad (3b)$$

where the single and double primes denote the TE- and TM-polarized waves, respectively, k_{tmn} is the transverse propagation

vector, ρ is the transverse coordinate vector, and $\underline{a}'_{mn}$ and $\underline{a}''_{mn}$ are unit vectors related to transverse propagation constant by

$$\underline{a}'_{mn} = \frac{\underline{k}_{tmn}}{k_{tmn}} \tag{4a}$$

$$\underline{a}''_{mn} = \underline{z}_o \times \underline{a}'_{mn} = \frac{\underline{z}_o \times \underline{k}_{tmn}}{k_{tmn}} \tag{4b}$$

with

$$\underline{k}_{tmn} = k_{xm}\underline{x}_o + k_{yn}\underline{y}_o \tag{5a}$$

$$k_{xm} = k_o \sin\theta\cos\phi + \frac{2m\pi}{a} \tag{5b}$$

$$k_{yn} = k_o \sin\theta\sin\phi + \frac{2n\pi}{b}. \tag{5c}$$

Here, k_{xm} and k_{yn} are the propagation constants of the mth space harmonic in the x-direction and the nth space harmonic in the y-direction, respectively. And k_o is the propagation constant of the plane wave in the incident region, while θ and ϕ are the elevation and azimuthal angles of the incident wave in the spherical coordinate, respectively. x_o, y_o, and z_o, stand for the three unit base vectors of the rectangular coordinate system. Furthermore, the Vs and Is represent the vertical variations of the electric and magnetic fields of the mnth harmonics, respectively, and can be written generally as a superposition of the forward and backward traveling waves as

$$V_{mn}(z) = f_{mn}\exp(-jk_{zmn}z) + g_{mn}\exp(+jk_{zmn}z) \tag{6a}$$

$$I_{mn}(z) = Y_{mn}[f_{mn}\exp(-jk_{zmn}z) - g_{mn}\exp(+jk_{zmn}z)] \tag{6b}$$

where f_{mn} and g_{mn} are the amplitudes of the forward and backward traveling waves, respectively. It is noted that the primes over the field quantities are omitted here for simplicity; these expressions hold for either singly or doubly primed quantities, denoting the TE- and TM-polarized fields. Finally, k_{zmn} and Y_{mn} are the longitudinal propagation constant and the wave admittance of the mnth harmonic in air region, respectively, and they are given by

$$k_{zmn} = \sqrt{k_o^2 - k_{xm}^2 - k_{yn}^2} \tag{7a}$$

$$Y_{mn} = \begin{cases} \dfrac{k_{zmn}}{\omega\mu_o}, & \text{for TE modes} \\[2mm] \dfrac{\omega\varepsilon_o}{k_{zmn}}, & \text{for TM modes}. \end{cases} \tag{7b}$$

So far, all the parameters needed for the field representations in (3) have been defined and what remains to be determined is the set of amplitudes of the backward traveling waves gs for a given set of amplitudes of the incident waves that travel in the forward direction, fs in (6).

With the EM fields of each space harmonic represented above, the total EM fields in the air region can then be written as a superposition of all the space harmonics and they are then required to satisfy the boundary condition at the periodic impedance surface at $z = 0$

$$\underline{z}_o \times \underline{E}(\rho, z = 0) = Z_s(x, y)\underline{H}(\rho, z = 0). \tag{8}$$

In the Appendix, it is shown in mathematical details that the above boundary condition yields a set of linear matrix equations

$$\underline{V}'(0) = Z_s[\boldsymbol{D}^{(1,1)}\underline{I}'(0) + \boldsymbol{X}^{(1,2)}\underline{I}''(0)] \tag{9a}$$

$$\underline{V}''(0) = Z_s[\boldsymbol{X}^{(2,1)}\underline{I}'(0) + \boldsymbol{D}^{(2,2)}\underline{I}''(0)] \tag{9b}$$

where the $\boldsymbol{D}$s and $\boldsymbol{X}$s are matrices related to the structural as well as the incident-wave parameters and the Vs and Is are unknown vectors to be determined.

Let $\underline{f}'_{mn}$ and $\underline{f}''_{mn}$ be the amplitudes of the incident TE and TM modes, respectively, and let $\underline{g}'_{mn}$ and $\underline{g}''_{mn}$ be those of the reflected modes in air region. At $z = 0$, the voltage and current waves vectors are given by

$$\underline{V}(0) = \underline{f} + \underline{g} \tag{10a}$$

$$\underline{I}(0) = Y^{(a)}(\underline{f} - \underline{g}) \tag{10b}$$

where $Y^{(a)}$ is the admittance matrix in the air region. $\underline{f}$ is a supervector with $\underline{f}'$ and $\underline{f}''$ as its subvectors that are formed by a'_{mn} and a''_{mn} as their mnth elements, respectively, and similarly for g. From (9) and (10), we can obtain the relationship between f and g:

$$\underline{g} = \Gamma\underline{f} \tag{11}$$

where Γ is the reflection matrix of the 2-D periodic impedance surface. Here, $\underline{f}$ is supposed to be a known column vector for a given set of the incident space harmonics; with the reflection matrix computed, $\underline{g}$ is determined by (11) for the amplitudes of the space harmonics reflected from the periodic impedance surface back into the air region.

IV. NUMERICAL RESULTS AND DISCUSSIONS

Based on the exact formulation described in the preceding section, we are now in a position to carry out both qualitative and quantitative analysis of scattering characteristics of the 2-D periodic impedance surface. First, we shall invoke the concept of small perturbation to develop approximation techniques by which the first-order solutions can be constructed conveniently. This allows us to identify in an easy manner various physical effects associated with the structure in hand and this will be particularly useful for practical design considerations. Second, for a numerical analysis, the infinite system of equations for the Fourier amplitudes has to be truncated to a finite order and the numerical accuracy has to be carefully studied. It should be noted that it would be essential to employ techniques to ensure the more rapid convergence of the numerical process for the truncation of the resulting infinite matrix [22], [23]. After the numerical accuracy is assured, extensive numerical data are obtained to identify systematically all possible physical processes associated with the structure under investigation and to explore potential applications. We present here some numerical results from a parametric study on the general characteristics of plane-wave scattering by 2-D periodic impedance surface.

For the numerical analysis in this section, the two periods in x- and y-direction are chosen to be identical. The lossy surface

impedance is chosen to be $Z_s = 0.001 + j0.5$ (normalized to the wave impedance of the plane wave in the free space). Finally, the modulation indexes are chosen to be $\delta_x = \delta_x = 0.1$ and $\delta_{xy} = 0.05$. We shall investigate the effect of the elevation angle, the azimuth angle, and the wavelength of the incident wave.

Before embarking on an elaborate computations, it is instructive to examine first the limiting case of vanishing modulation indexes $\delta_x = \delta_y = \delta_{xy} = 0$. In the absence of the periodic perturbations, we have a uniform impedance surface for which the guiding characteristics are well known. In particular, for a lossless reactive surface, the propagation constant of the surface wave is given explicitly by

$$k_{sw}^2 = k_x^2 + k_y^2 = k_o^2 n_{sw}^2 \tag{12}$$

$$n_{sw}^2 = \begin{cases} 1 + \dfrac{1}{X_s^2}, & \text{for TE mode with } X_s < 0 \\ 1 + X_s^2, & \text{for TM mode with } X_s > 0 \end{cases} \tag{13}$$

where X_s is the surface reactance normalized to the free-space wave impedance $Z_o = 120\,\pi\,\Omega$. n_{sw} may be interpreted as the effective refractive index of the surface wave. It is noted that the TE surface wave exists only for capacitive surface and TM surface wave for inductive surface. In such a special case, the dispersion curve representing the relationship between k_x and k_y is a circle of the radius k_{sw}.

We have carried out considerable numerical experiments with various parameters of the incident wave as well as the 2-D periodic impedance surface; however, only a few sets are selected here to exhibit the interesting phenomena that may take place in the presence of a 2-D periodic impedance surface. Figs. 4 and 5 shows the reflected intensity versus wavelength λ of the incident wave, for the incident angle $\theta = 30°$ and $\phi = 0°$. The designations of the curves are as follows: the solid line is for the reflection efficiency with copolarization (TE–TE or TM–TM), while the dashed line is for that of cross polarization (TE–TM or TM–TE). Furthermore, we observe that there exist many regions of sharp variation along the curves, as marked by the characters from A to F in Figs. 4 and 5.

To explain the unusual behavior of reflection characteristics, we recall that the normalized transverse propagation constant can be obtained from (5) as

$$\frac{k_{tmn}}{k_o} = \sqrt{\left(\sin\theta\cos\phi + m\frac{\lambda}{a}\right)^2 + \left(\sin\theta\sin\phi + n\frac{\lambda}{b}\right)^2}. \tag{14}$$

Graphically, the transverse propagation constant are plotted in Fig. 6, for the eight diffracted orders: $(m = +1, n = 0)$, $(m = -2, n = +1)$, $(m = -2, n = -1)$, $(m = -2, n = 0)$, $(m = 0, n = -1)$, $(m = 0, n = +1)$, $(m = -1, n = -1)$, and $(m = -1, n = +1)$. It is noted that for $\phi = 0°$, some harmonics may follow the same curve with multiple labels. Furthermore, the propagation constant of the surface wave given by (13) is plotted in the long-dashed line and so is the cutoff condition with the short-dashed line. Here, we have nine intersection points between the set of solid lines and the long-dashed line as marked in alphabetical order from A to I according to
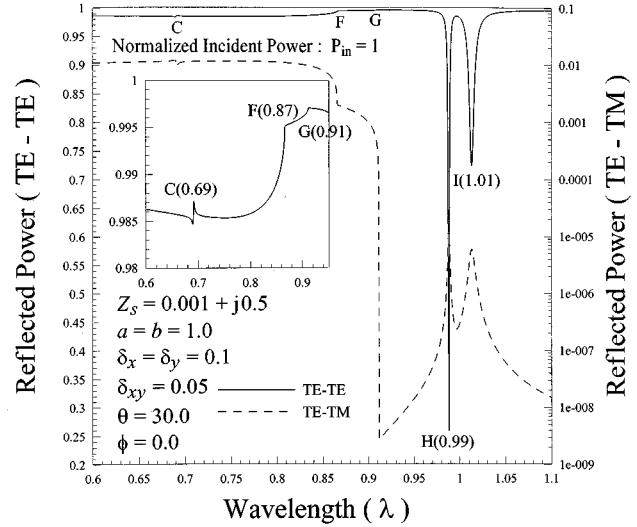

Fig. 4.   Variation of reflected power versus wavelength; TE plane wave incidence.
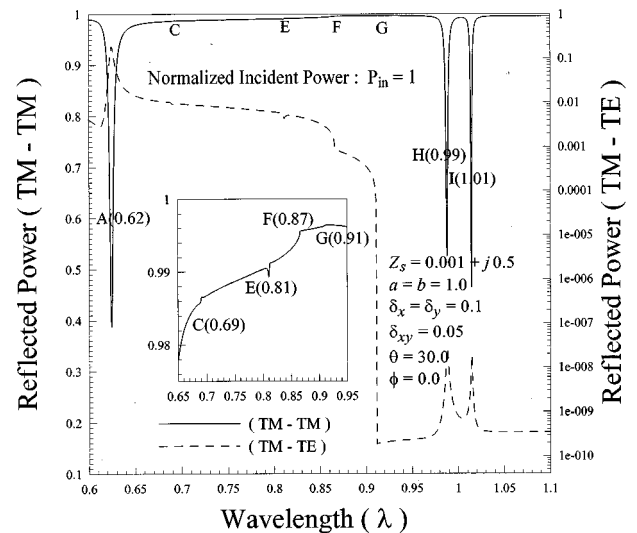

Fig. 5.   Variation of reflected power versus wavelength; TM plane wave incidence.

the frequency. Among these intersection points, A, C, E, H, and I determine the frequencies for the conditions of the phase matching between the harmonics and the guided wave. Hence, it is expected that strong couplings from the incident wave to the guided wave may take place in the vicinities of these points. With the resistive loss of the impedance surface, such couplings result in the anomalous absorption, as will be further discussed. On the other hand, the intersection points B, D, F, and G determine the cutoff conditions of various space harmonics and some strong reactions should be expected in the vicinities of these points. Finally, it is interesting to observe that the two points designated by the H and I actually coincide with each other. Judging from the curves, a coflow passive coupling or directional coupling should take place there; therefore, the two point should split, with one at a wavelength slightly smaller and the
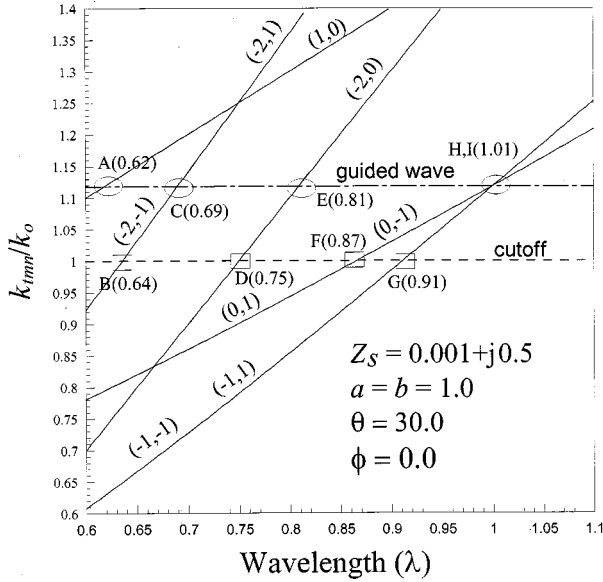
Fig. 6. Variation of transverse wavenumber versus wavelength for various space harmonics.

other slightly greater than 1.0. With these predictions based on physical intuition, we can explain easily the scattering characteristics of the periodic impedance surface.

We observe that there exist sharp variations of the reflected power at some wavelengths, as marked by C, F, G, H, and I, for the TE-incidence case. It is noted that the number inside the parentheses after each character indicates the exact wavelength. On the other hand, Fig. 5 shows that in addition to those at the wavelengths marked in Fig. 4, there are sharp variations at two more wavelengths, as marked by A and E, for the TM-incidence case. By inspection, every wavelength marked in Figs. 4 and 5 can be identified clearly with those wavelengths marked in Fig. 6, except the two points B and D at which no sharp reaction to the incident wave is observed. The physical explanation of these phenomena are given below.

Consider first the coupling of an incident wave to the guided wave. It is recalled that for the parameters under consideration, the structure supports only the TM surface wave. We observe that corresponding to the intersection point A and E in Fig. 6, the direct coupling from an incident wave to the guided wave can take place only with a TM incidence case, but not otherwise. Furthermore, for the special case of the incident angle $\phi = 0°$, the propagation constant in the y-direction is equal to zero for two harmonics $(m = 1, n = 0)$ and $(m = -2, n = 0)$. This means the uniformity in the y-direction of the fields associated with these harmonics and the cross-polarization coupling to the guided wave should be of a higher order effect and its effect on the scattering characteristics does not show up in the case of the TE incidence. This explains the sharp variations marked by A and E appearing in Fig. 5 for TM incidence case, but not in Fig. 4 for TE incidence case. It is interesting to observe that in the scattering results, the two points H and I do split sufficiently far apart in wavelength due to the coflow coupling between two set of harmonics, as expected.

For the cutoff conditions at the points B, D, F, and G in Fig. 6, we observe that those at points B and D do not have any visible effect on reflected power in either Fig. 4 or 5. This can be attributed to the fact that the harmonics involved are of the higher order and the effect should be small. On the other hand, the variations in the vicinities of the points marked by F and G are quite pronounced, is evident in both Figs. 4 and 5. These are due to the cutoff conditions of the lower order space harmonics $(m = 0, n = \pm 1)$ and $(m = -1, n = \pm 1)$ and are known as the phenomena of Wood's anomaly of the Raleigh type.

Although not shown here, we have also performed calculations for the reflected power under various conditions. However, the general behavior of the anomalous absorption as a function of the incident elevation and azimuth angles is similar to those in Figs. 4 and 5 and they are not shown. In summary, the plots of the dispersion curve, the cutoff condition and the wavenumbers for the relevant harmonics are very easy to do and this provides a plausible physical basis for the investigation of the plane wave scattering by a periodic impedance surface, as demonstrated above.

V. CONCLUSION

We have presented a rigorous treatment to the 3-D boundary-value problem of plane wave scattering by a planar 2-D periodic impedance surface since the 2-D periodic structure is replaced by a 2-D periodic IBC on a virtual surface. The formulation of the problem is based on the rigorous method of mode matching. Numerical results are systematically carried out to illustrate the reflected characteristics; in particular, Wood's anomalies associated with 2-D periodic impedance surface are carefully examined and are shown to provided a mechanism for the anomalous absorption of incident wave. Most importantly, the additional periodicity in the y-direction may results in more coupling conditions between space harmonics and surface wave supported by the impedance surface. As an example, this mechanism may be employed to reduce the radar cross section in further study.

APPENDIX

We have shown that the tangential electric and magnetic fields in the air have been expressed as a superposition of plane waves as given by (3) and (4); to repeat, they are

$$\underline{z}_o \times \underline{E}_t(\underline{\rho}, z) = \sum_{m,n} [\underline{a}'_{mn} \cdot V'_{mn}(z) + \underline{a}''_{mn} \cdot V''_{mn}(z)] \cdot \varphi_{mn}$$

$$\text{(A.1)}$$

$$\underline{H}_t(\underline{\rho}, z) = \sum_{m,n} [\underline{a}'_{mn} \cdot I'_{mn}(z) + \underline{a}''_{mn} \cdot I''_{mn}(z)] \cdot \varphi_{mn}$$

$$\text{(A.2)}$$

$$\varphi_{mn} = \exp(-j\underline{k}_{tmn} \cdot \underline{\rho})$$

Substituting (A.1) and (A.2) into (A.3) and then, taking the inner product with $\underline{a}'_{m,n}$ on both sides of the resulting equality, we

obtain the following relationships between the harmonic amplitudes of the voltage and current:

$$
\begin{aligned}
V'_{m,n}&(0)\\
&= Z_s \sum_{m,n} \Big\{ \big[I'_{mn}(0) + \delta_x \\
&\quad \cdot \Big[K^{(1,1)}_{m-1,n} I'_{m-1,n}(0) + K^{(1,2)}_{m-1,n} I''_{m-1,n}(0) \Big] \\
&\quad + \delta_x \Big[K^{(1,1)}_{m+1,n} I'_{m+1,n}(0) + K^{(1,2)}_{m+1,n} I''_{m+1,n}(0) \Big] \\
&\quad + \delta_y \Big[K^{(1,1)}_{m,n-1} I'_{m,n-1}(0) + K^{(1,2)}_{m,n-1} I''_{m,n-1}(0) \Big] \\
&\quad + \delta_y \Big[K^{(1,1)}_{m,n+1} I'_{m,n+1}(0) + K^{(1,2)}_{m,n+1} I''_{m,n+1}(0) \Big] \\
&\quad + \delta_{xy} \Big[K^{(1,1)}_{m-1,n-1} I'_{m-1,n-1}(0) \\
&\qquad\qquad + K^{(1,2)}_{m-1,n-1} I''_{m-1,n-1}(0) \Big] \\
&\quad + \delta_{xy} \Big[K^{(1,1)}_{m-1,n+1} I'_{m-1,n+1}(0) \\
&\qquad\qquad + K^{(1,2)}_{m-1,n+1} I''_{m-1,n+1}(0) \Big] \\
&\quad + \delta_{xy} \Big[K^{(1,1)}_{m+1,n-1} I'_{m+1,n-1}(0) \\
&\qquad\qquad + K^{(1,2)}_{m+1,n-1} I''_{m+1,n-1}(0) \Big] \\
&\quad + \delta_{xy} \Big[K^{(1,1)}_{m+1,n+1} I'_{m+1,n+1}(0) \\
&\qquad\qquad + K^{(1,2)}_{m+1,n+1} I''_{m+1,n+1}(0) \Big]
\end{aligned} \tag{A.3}
$$

for $m, n = -\infty .. + \infty$

where

$$
K^{(1,1)}_{m\pm 1, n\pm 1} = \left\langle \underline{a'}_{m,n} \big| \underline{a'}_{m\pm 1, n\pm 1} \right\rangle \tag{A.4}
$$

and

$$
K^{(1,2)}_{m\pm 1, n\pm 1} = \left\langle \underline{a'}_{m,n} \big| \underline{a''}_{m\pm 1, n\pm 1} \right\rangle . \tag{A.5}
$$

We may now fix the integer m and group the harmonics according to the index n to form the new vector relationship

$$
\begin{aligned}
Y_s \underline{V'}_m(0) &= \boldsymbol{D}^{(1,1)}_m \underline{I'}_m(0) + \boldsymbol{K}^{(1,1)}_{m+1} \underline{I'}_{m+1}(0) + \boldsymbol{K}^{(1,1)}_{m-1} \underline{I'}_{m-1}(0) \\
&\quad + \boldsymbol{X}^{(1,2)}_m \underline{I''}_m(0) + \boldsymbol{K}^{(1,2)}_{m+1} \underline{I''}_{m+1}(0) + \boldsymbol{K}^{(1,2)}_{m-1} \underline{I''}_{m-1}(0).
\end{aligned} \tag{A.6}
$$

Similarly, taking the inner product with $\underline{a''}_{m,n}$ and performing the same process as the above, we obtain

$$
\begin{aligned}
Y_s \underline{V''}_m(0) &= \boldsymbol{D}^{(2,2)}_m \underline{I''}_m(0) + \boldsymbol{K}^{(2,2)}_{m+1} \underline{I''}_{m+1}(0) + \boldsymbol{K}^{(2,2)}_{m-1} \underline{I''}_{m-1}(0) \\
&\quad + \boldsymbol{X}^{(2,1)}_m \underline{I'}_m(0) + \boldsymbol{K}^{(2,1)}_{m+1} \underline{I'}_{m+1}(0) + \boldsymbol{K}^{(2,1)}_{m-1} \underline{I'}_{m-1}(0)
\end{aligned} \tag{A.7}
$$

where $\underline{V'}_m(0)$, $\underline{I'}_m(0)$ and $\underline{I''}_m(0)$ are column vectors with $V_{mn}(0)$ and $I_{mn}(0)$ as their nth elements, respectively, and matrices $D^{(1,1)}_m$, $X^{(1,2)}_m$, $K^{(1,1)}_{m\pm 1}$ and $K^{(1,2)}_{m\pm 1}$ are matrices related

to the structural as well as the incident parameters. Finally, expressing them in the form of supermatrix and supervector by collecting all the elements according to the index m in (A.6) and (A.7), we have the desired results shown in (9).

ACKNOWLEDGMENT

REFERENCES

[1] T. Tamir, H. C. Wang, and A. A. Oliner, "Wave propagation in sinusoidally stratified dielectric media," *IEEE Trans. Microwave Theory Tech.*, vol. MTT-12, pp. 323–335, 1964.

[2] Hessel and A. A. Oliner, "A new theory of Wood's anomalies on optical gratings," *Appl. Opt.*, vol. 4, pp. 1275–1297, 1965.

[3] S. T. Peng, T. Tamir, and H. L. Bertoni, "Theory of dielectric grating waveguides," *IEEE Trans. Microwave Theory Tech.*, vol. MTT-23, pp. 123–133, 1975.

[4] Elach, "Wave in active and passive periodic structures: A review," *Proc. IEEE*, vol. 64, pp. 1666–1698, 1976.

[5] J. C. Vardaxoglou, A. Hossainzadeh, and A. Stylianou, "Scattering from two-layer FSS with dissimilar lattice geometries," *Inst. Elect. Eng. Proc. Microwaves, Antennas, Propagat.*, pt. H, vol. 140, pp. 59–61, Feb. 1993.

[6] T. K. Wu, *Frequency Selective Surface and Grid Array*. New York: Wiley, 1995.

[7] C. Scott's, *The Spectral Domain Method in Electromagnetics*. Norwell, MA: Artech House, 1989.

[8] D. Maystre, "Electromagnetic study of photonic band gaps," *Pure Appl. Opt.*, vol. 3, no. 6, pp. 975–993, Nov. 1994.

[9] V. Radisic, Y. Qian, R. Coccioli, and T. Itoh, "Novel 2-D photonic bandgap structure for microstrip lines," *IEEE Microwave Guided Wave Lett.*, vol. 8, pp. 69–71, Feb. 1998.

[10] H. Y. David Yang, "Finite difference analysis of 2-D photonic crystals," *IEEE Trans. Microwave Theory Tech.*, vol. 44, pp. 2688–2695, Dec. 1996.

[11] *Electromagnetic Theory of Gratings: Theory of Crossed Gratings*. New York: Springer-Verlag, 1980, ch. 7.

[12] R. C. Hall, R. Mittra, and K. M. Mitzner, "Analysis of multilayered periodic structures using generalized scattering matrix theory," *IEEE Trans. Antennas Propagat.*, vol. 36, pp. 511–517, Apr. 1988.

[13] E. Noponen and J. Turunen, "Eigenmode method for electromagnetic synthesis of diffractive elements with three-dimensional profiles," *J. Opt. Soc. Amer. A*, vol. 11, no. 9, pp. 2494–2502, 1994.

[14] R. B. Hwang and S. T. Peng, "Performance evaluation of bigratings as a beam splitter," *Appl. Opt.*, vol. 36, pp. 2011–2018, 1997.

[15] L. Zhang and N. G. Alexopoulos, "Thin frequency-selective lattices in novel compact MIC, MIMIC, and PCA architectures," *IEEE Trans. Microwave Theory Tech.*, vol. 46, pp. 1936–1948, Nov. 1998.

[16] J. R. Wait, "The scope of impedance boundary conditions in radio propagation," *IEEE Trans. Geosci. Remote Sensing*, vol. 28, pp. 721–723, July 1990.

[17] T. B. A. Senior and J. L. Volakis, "Generalized impedance boundary conditions in scattering," *Proc. IEEE*, vol. 79, pp. 1413–1420, Oct. 1991.

[18] T. B. A. Senior and J. L. Volakis, "Derivation and application of a class of generalized boundary conditions," *IEEE Trans. Antennas Propagat.*, vol. 37, pp. 1566–1572, Dec. 1989.

[19] D. J. Hoppe and Y. Rahmat-Samii, *Impedance Boundary Conditions in Electromagnetics*. Bristol, U.K.: Taylor Francis, 1995.

[20] R. B. Hwang and S. T. Peng, "Guidance characteristics of two-dimensional periodic impedance surface," *IEEE Trans. Microwave Theory Tech.*, vol. 47, pp. 2503–2511, 1999.

[21] T. Su and H. Ling, "Determining the equivalent impedance boundary condition for material coated corrugated gratings based on the genetic algorithm," in *Proc. Int. Symp. Antennas Propagat. Soc. Dig.*, Atlanta, GA, June 1998, pp. 38–41.

[22] E. Michielssen and R. Mittra, "Scattering from dielectric and periodic profiles characterized by an impedance boundary condition," in *Int. Symp. Antennas Propagat. Soc. Dig.*, London, ON, Canada, June 1991, pp. 280–283.

[23] K. Sarabandi, "Scattering from variable resistive and impedance sheets," *J. Electromagn. Waves Applicat.*, vol. 4, no. 9, pp. 865–891, 1990.

[24] W. Rotman, "A study of single-surface corrugated guides," *Proc. IRE*, vol. 39, p. 952, 1951.

[25] R. Elliot, "On the theory of corrugated plane surface," *IRE Trans. Antennas Propagat.*, pt. 2, pp. 71–78, July 1954.

[26] S. Lee and W. Jones, "Surface waves on two-dimensional corrugated surfaces," *Radio Sci.*, vol. 6, pp. 811–817, 1971.

Ruey Bing Hwang (M'96) was born in Nan-Tou, Taiwan, on January 20, 1967. He received the B.S. degree in communication engineering from National Chiao-Tung University, Hsinchu, Taiwan, R.O.C., in 1990, the M.S. degree from the Institute of Electrical Engineering, National Taiwan University Taipei, Taiwan, R.O.C., in 1992, and the Ph.D. degree from the Institute of Electronics, National Chiao-Tung University, Hsinchu, Taiwan, R.O.C., in 1996.

From 1996 to 1999, he was with the National Center for High-Performance Computing, Hsinchu, Taiwan, R.O.C, where he worked on computational electromagnetics. In the summer of 1999, he joined the Microelectronics and Information Systems Research Center, National Chiao-Tung University, Hsinchu, Taiwan, R.O.C., as an Associate Researcher. His professional interests include guidance and scattering characteristics of periodic structures, antenna design, and electromagnetic compatibility.

Dr. Hwang is a member of Phi Tau Phi.